

Supplementary Information

Layered Ferrimagnets Constructed from Charge-Transferred Paddlewheel [Ru₂] Units and TCNQ Derivatives: The Importance of Interlayer Translational Distance in Determining Magnetic Ground State

Wataru Kosaka,^{ab} Zhaoyuan Liu^b, and Hitoshi Miyasaka^{*ab}

^a Institute for Materials Research, Tohoku University, 2-1-1 Katahira, Aoba-ku Sendai, Miyagi 980-8577, Japan

^b Department of Chemistry, Graduate School of Science, Tohoku University, 6-3 Aramaki-Aza-Aoba, Aoba-ku, Sendai, Miyagi 980-8578, Japan

e-mail: miyasaka@imr.tohoku.ac.jp

Corresponding author*

Prof. Dr. Hitoshi Miyasaka

Institute for Materials Research, Tohoku University, 2–1–1 Katahira, Aoba-ku, Sendai, Miyagi 980-8577, Japan

E-mail: miyasaka@imr.tohoku.ac.jp

Tel: +81-22-215-2030

FAX: +81-22-215-2031

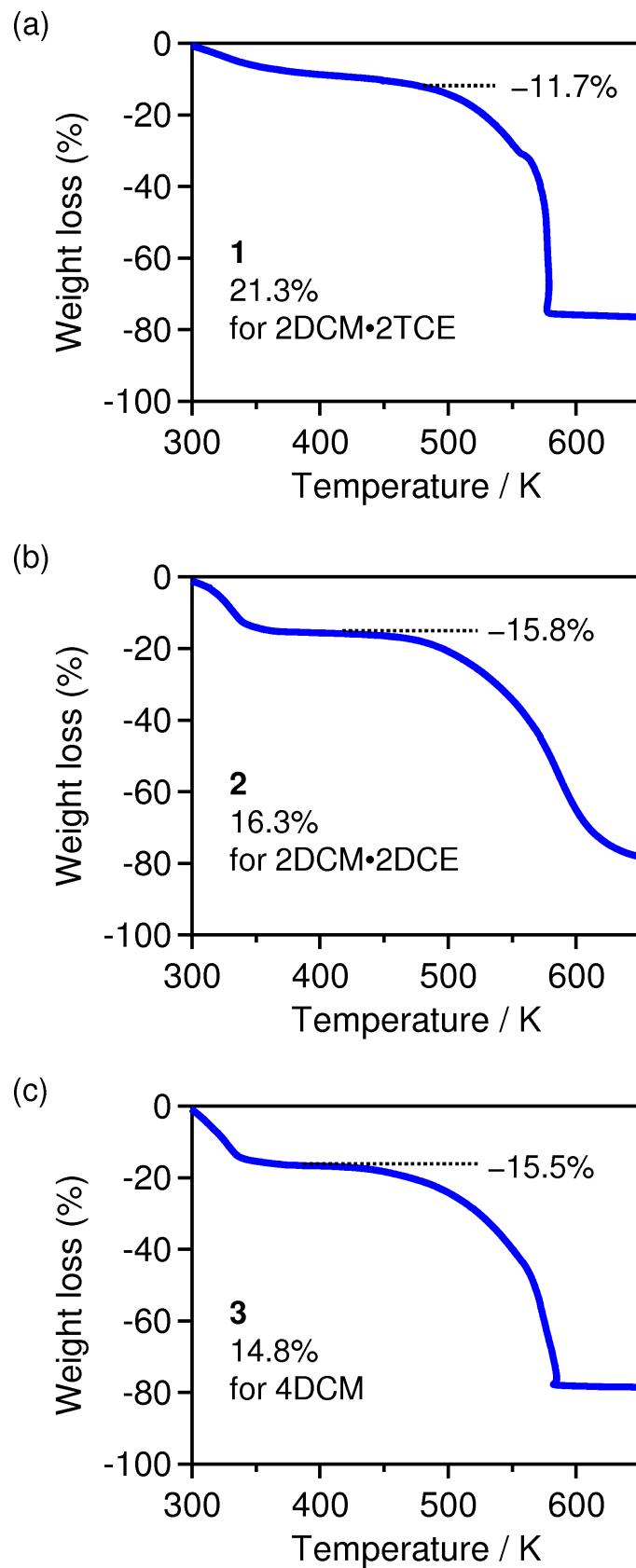


Fig S1. Thermal gravimetric analysis (TGA) profiles for **1** (a), **2** (b), and **3** (c) with a heating rate of 5 K min^{-1} under N_2 atmosphere.

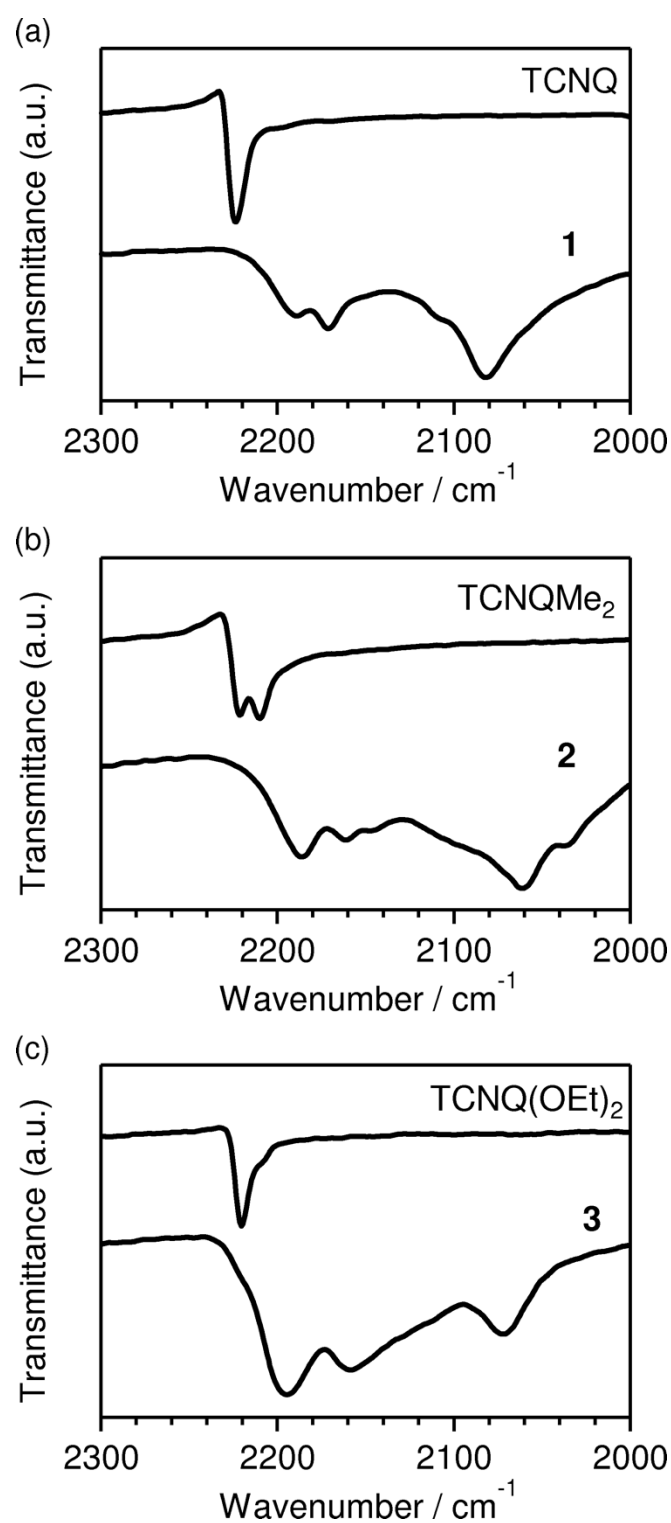


Fig. S2 Infrared spectra in the range of 2000–2300 cm^{-1} for **1** and TCNQ (a), **2** and TCNQMe₂ (b), and **3** and TCNQ(OEt)₂ (c) measured on KBr pellets at room temperature.

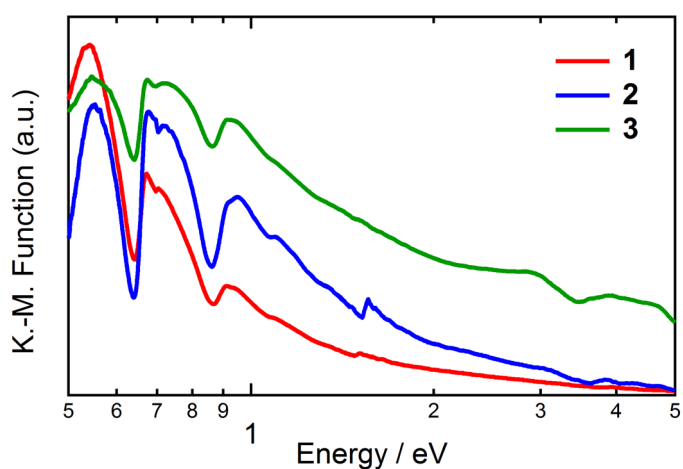


Fig. S3 Powder reflection spectra of **1–3** measured on pellets diluted with BaSO₄.

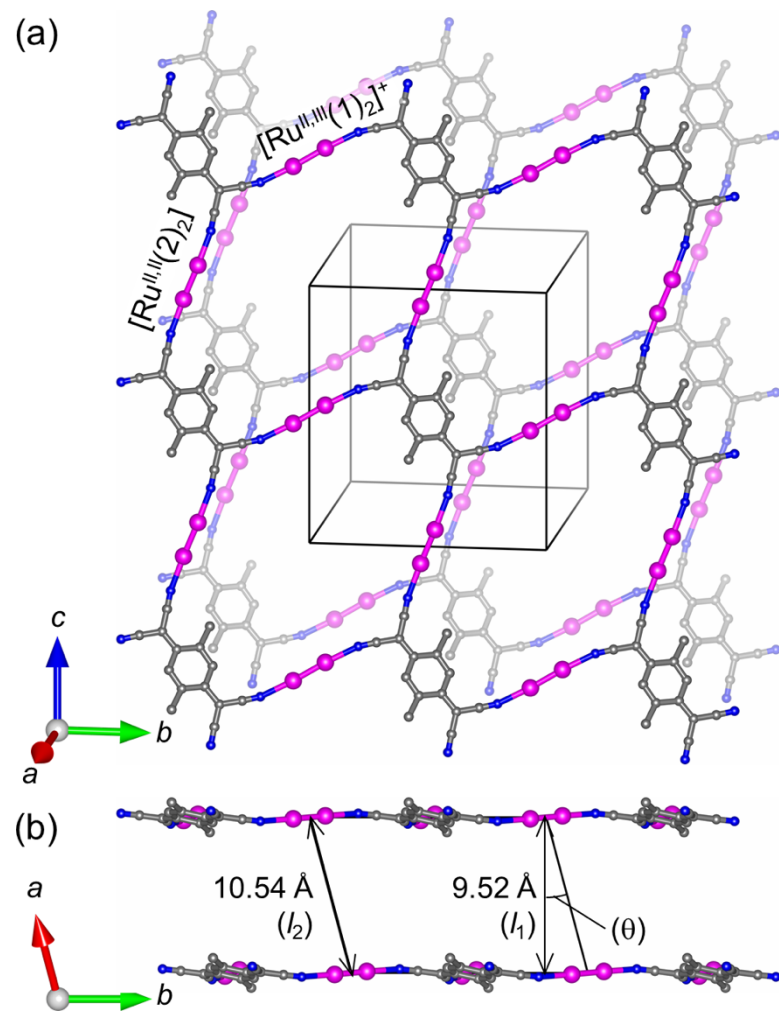


Fig. S4 Packing diagrams projected for **2** along $(1\ 0\ 0)$ plane (a) and c axis (b), where C, N, and Ru atoms are represented in gray, blue, and purple, respectively. Equatorial carboxylate ligands for $[Ru_2]$ units, crystallization solvents, and hydrogen atoms are omitted for clarity. l_1 and l_2 in Fig.b are defined by the vertical distance and the nearest $[Ru_2] \cdots [Ru_2]$ distance between $(1\ 0\ 0)$ planes, respectively.

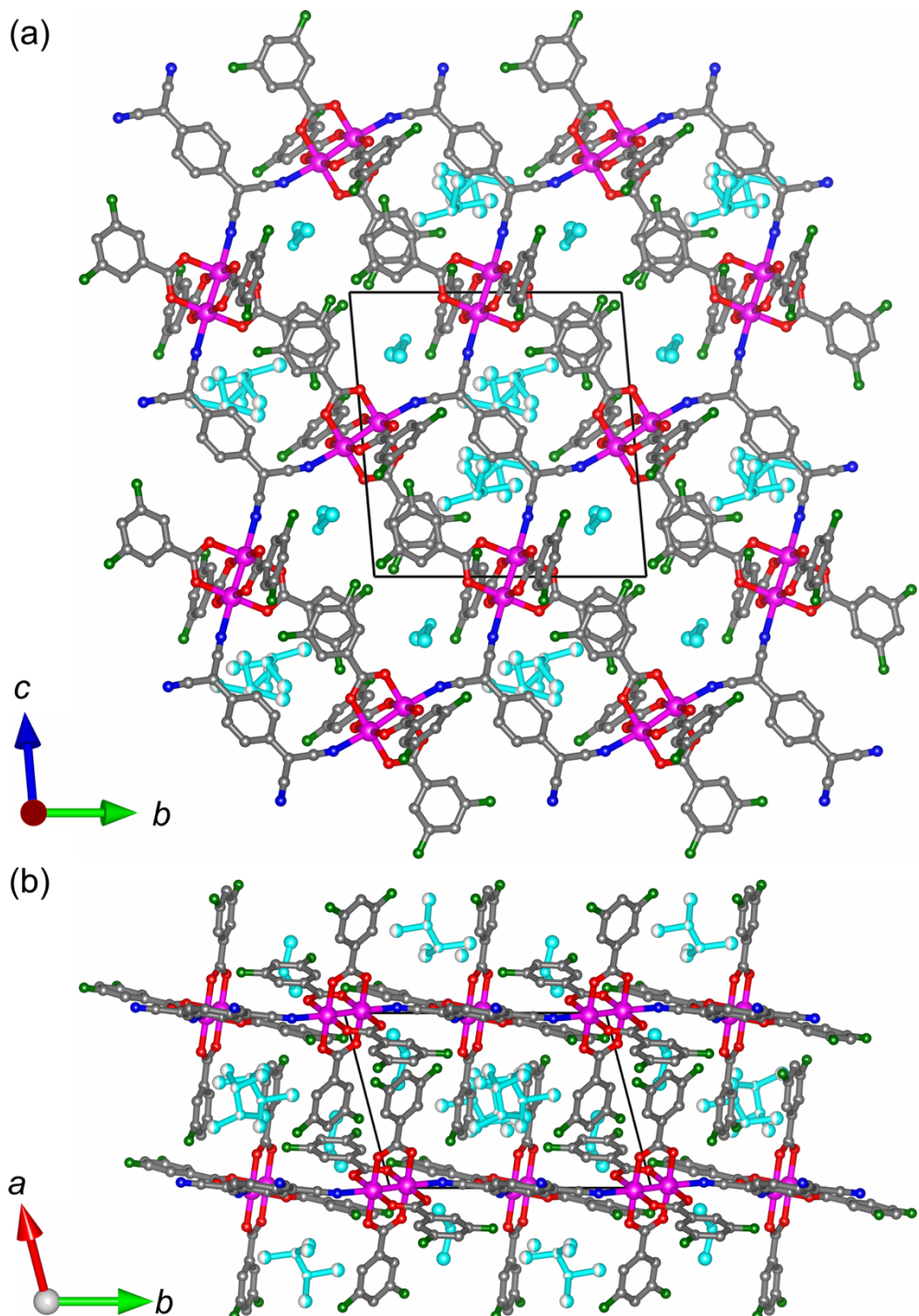


Fig. S5 Packing diagrams of **1**. A view along *a*-axis (a) and *c*-axis (b), where atoms C, N, O, F and Ru are represented in gray, blue, red, green, and purple, respectively. Crystallization solvents are depicted in cyan. Hydrogen atoms are omitted for clarity.

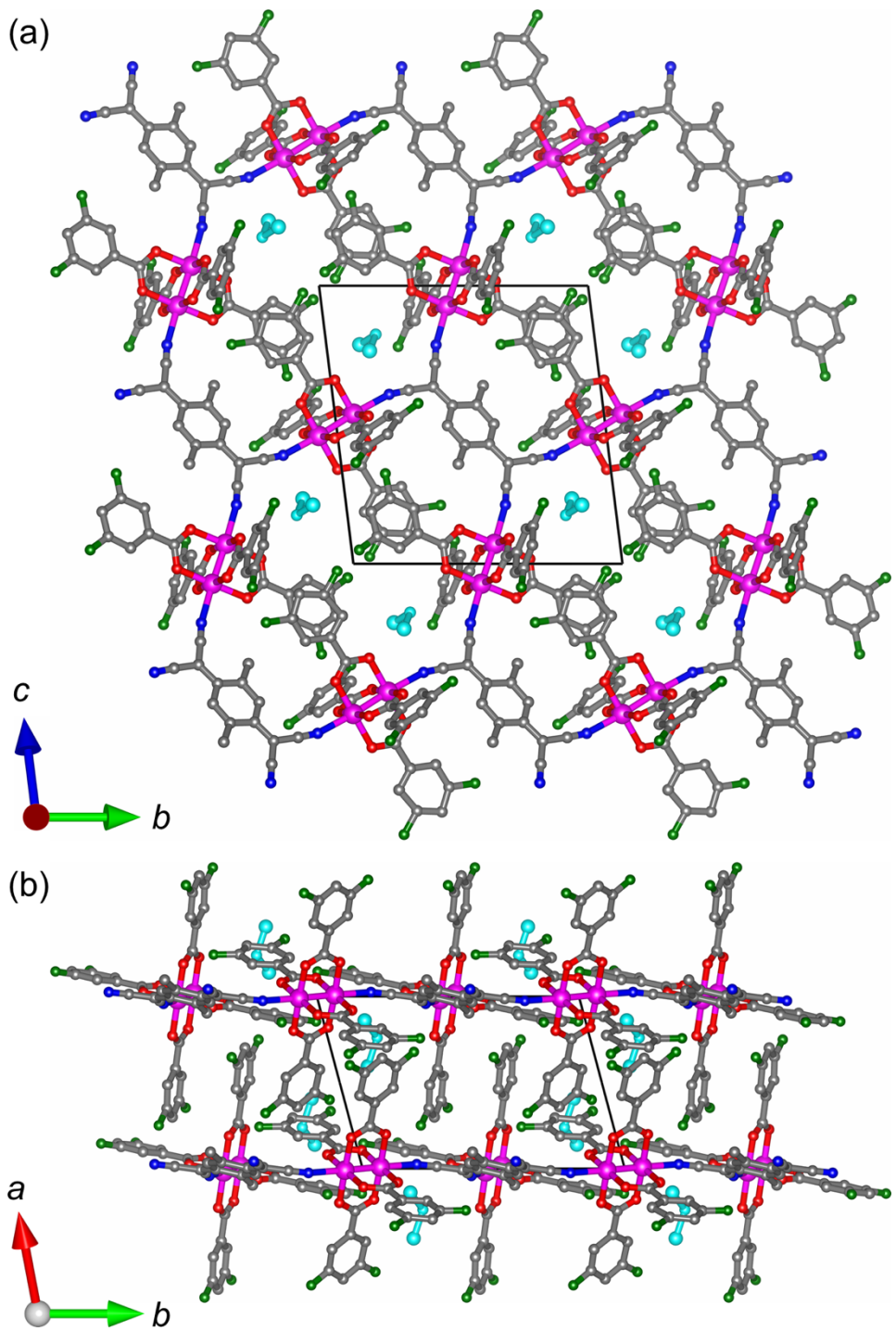


Fig. S6 Packing diagrams of **2**. A view along *a*-axis (a) and *c*-axis (b), where atoms C, N, O, F and Ru are represented in gray, blue, red, green, and purple, respectively. Crystallization solvents are depicted in cyan. Hydrogen atoms are omitted for clarity.

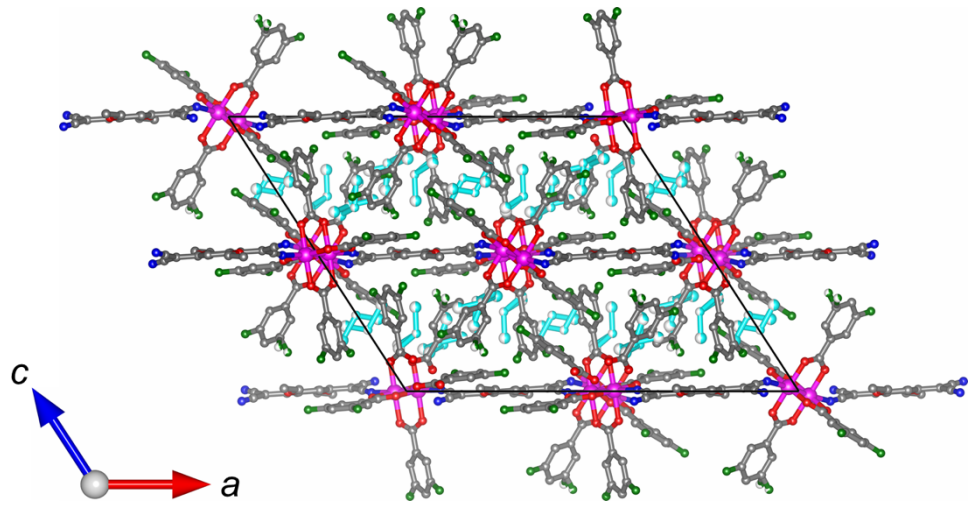


Fig. S7 Packing diagrams of **3** *b*-axis, where atoms C, N, O, F and Ru are represented in gray, blue, red, green, and purple, respectively. Crystallization solvents are depicted in cyan. Hydrogen atoms are omitted for clarity.

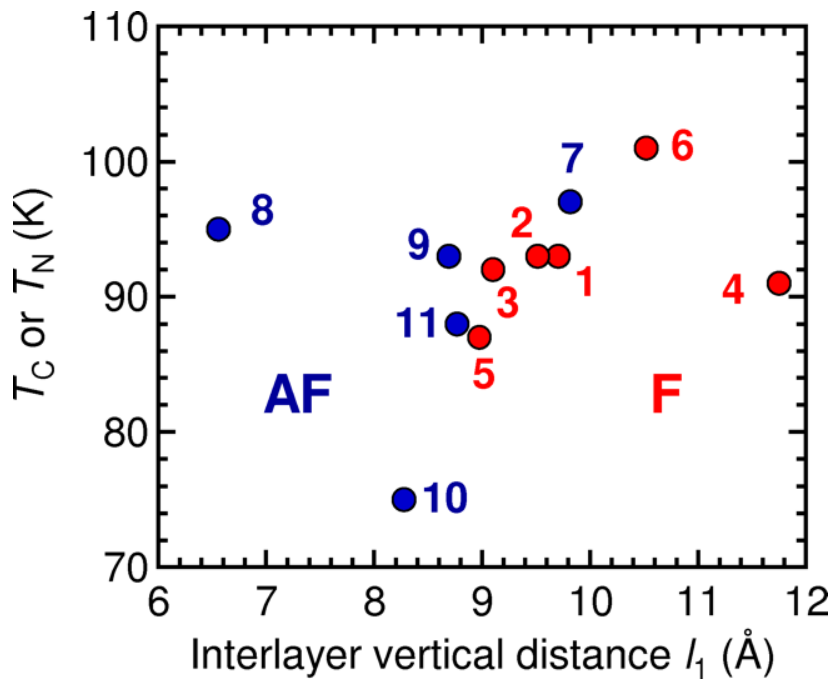


Fig. S8 Magnetic phase transition temperature (T_C or T_N) vs. interlayer vertical distance (l_1 , Fig. 2) plots for **1–3** and reported $[\text{Ru}_2]/\text{TCNQR}_x \text{ D}_2\text{A}$ system, where the compound with ferromagnetic and antiferromagnetic ground states are colored in red and blue, respectively: **4**, $[\{\text{Ru}_2(2,4,6\text{-F}_3\text{PhCO}_2)_4\}_2(\text{TCNQ})]\bullet 2\text{DCM}\bullet 2(p\text{-xylene})$; ¹ **5**, $[\{\text{Ru}_2(p\text{-FPhCO}_2)_4\}_2(\text{BTDA-TCNQ})]\bullet 2\text{DCM}\bullet 2(p\text{-chlorotoluene})$; ² **6**, $[\{\text{Ru}_2(2,3,5\text{-Cl}_3\text{PhCO}_2)_4\}_2(\text{TCNQMe}_2)]\bullet 4\text{DCM}$; ³ **7**, $[\{\text{Ru}_2(m\text{-ClPhCO}_2)_4\}_2\{\text{TCNQ}(\text{MeO})_2\}]\bullet 3.3\text{DCM}\bullet 2\text{TCE}$; ⁴ **8**, $[\{\text{Ru}_2(\text{CF}_3\text{CO}_2)_4\}_2(\text{TCNQF}_4)]\bullet 3(p\text{-xylene})$; ^{5,6,7} **9**, $[\{\text{Ru}_2(o\text{-FPhCO}_2)_4\}_2(\text{BTDA-TCNQ})]\bullet 4\text{DCM}$; ² **10**, $[\{\text{Ru}_2(o\text{-ClPhCO}_2)_4\}_2\{\text{TCNQ}(\text{MeO})_2\}]\bullet \text{DCM}$; ⁸ **11**, $[\{\text{Ru}_2(o\text{-FPhCO}_2)_4\}_2\{\text{TCNQ}(\text{MeO})_2\}]\bullet 4\text{DCM}$. ⁹

References in ESI

- (1) W. Kosaka, H. Fukunaga and H. Miyasaka, *Inorg. Chem.*, 2015, **54**, 10001–10006.
- (2) N. Motokawa, T. Oyama, S. Matsunaga, H. Miyasaka, M. Yamashita and K. R. Dunbar, *CrystEngComm*, 2009, **11**, 2121–2130.
- (3) J. Zhang, W. Kosaka, K. Sugimoto and H. Miyasaka, *J. Am. Chem. Soc.*, 2018, in press.
- (4) W. Kosaka, M. Itoh and H. Miyasaka, *Mater. Chem. Front.*, 2018, **2**, 497–504.
- (5) H. Miyasaka, T. Izawa, N. Takahashi, M. Yamashita and K. R. Dunbar, *J. Am. Chem. Soc.*, 2006, **128**, 11358–11359.
- (6) H. Miyasaka, N. Motokawa, S. Matsunaga, M. Yamashita, K. Sugimoto, T. Mori, N. Toyota and K. R. Dunbar, *J. Am. Chem. Soc.*, 2010, **132**, 1532–1544.
- (7) K. Nakabayashi, M. Nishio, K. Kubo, W. Kosaka and H. Miyasaka, *Dalton Trans.*, 2012, **41**, 6072–6074.
- (8) N. Motokawa, S. Matsunaga, S. Takaishi, H. Miyasaka, M. Yamashita and K. R. Dunbar, *J. Am. Chem. Soc.*, 2010, **132**, 11943–11951.
- (9) H. Fukunaga, T. Yoshino, H. Sagayama, J. Yamaura, T. Arima, W. Kosaka, H. Miyasaka, *Chem. Commun.*, 2015, **51**, 7795– 7798.